

Periodic and rational solutions of modified Korteweg-de Vries equation

Amdad Chowdury^a, Adrian Ankiewicz, and Nail Akhmediev

Optical Sciences Group, Research School of Physics and Engineering, The Australian National University, Canberra ACT 2600, Australia

Received 18 January 2016 / Received in final form 9 March 2016

Published online 12 May 2016 – © EDP Sciences, Società Italiana di Fisica, Springer-Verlag 2016

Abstract. We present closed form periodic solutions of the integrable modified Korteweg-de Vries equation (mKdV). By using a Darboux transformation, we derive first-and second-order doubly-periodic lattice-like solutions. We explicitly derive first-and second-order rational solutions as limiting cases of periodic solutions. We have also found the degenerate solution which corresponds to the equal eigenvalue case. Among the second-order solutions, we single out the doubly-localized high peak solution on a constant background with an infinitely extended trough. This solution plays the role of a rogue wave of the mKdV equation.

1 Introduction

The first observation of a solitary wave on a water surface was reported by the Scottish naval engineer J. Scott Russell back in the nineteenth century [1]. Theoretical analysis of such a wave was presented by British scientist Lord Rayleigh [2] and French scientist Boussinesq [3–6]. In 1895, two Dutch mathematicians, Korteweg and de Vries, formulated a partial differential equation (now known as the KdV equation) whose closed form solution precisely modelled the propagation of shallow water waves [7]. In fact, the ‘KdV’ equation and its fundamental soliton solution are explicitly given in the earlier Boussinesq’s paper [5], wherein “Scott Russell’s solitary wave” is also obtained. Numerical analysis of this equation by Zabuski and Kruskal [8] showed that a localized initial condition results in the excitation of solitons. Gardner et al. [9] were the first to solve an initial value problem involving the KdV equation using the inverse scattering theory with the one-dimensional Schrödinger operator.

The mKdV equation and its further modifications are found to describe pulses consisting of a few optical cycles [10–12] and in modelling supercontinuum generation in optical fibres [13]. The mKdV equation has many other applications in various fields such as soliton propagation in lattices [14], nonlinear Alfvén waves propagating in plasma [15] and meandering ocean currents [16]. It can also be applied to the dynamics of traffic flow [17–19]. Furthermore, the mKdV equation is related to Schottky barrier transmission lines [20], ion acoustic soliton experiments in plasmas [21] and fluid mechanics [22].

For convenience, we write the focussing mKdV equation in the following way:

$$\frac{\partial\psi}{\partial x} - \alpha \left(\frac{\partial^3\psi}{\partial t^3} + 6\psi^2 \frac{\partial\psi}{\partial t} \right) = 0, \quad (1)$$

where $\psi = \psi(x, t)$ is a real function with evolution variable x and transverse variable t . We explicitly retain an arbitrary real parameter, α , in the equation in order to have consistent notation with our previous results [23,24] and because it is useful at times. It can be removed by rescaling the x -variable: $\alpha x \rightarrow x'$. The equation containing the Hirota operator alone [25,26] differs from equation (1) in that ψ^2 in the third term is replaced by $|\psi|^2$ (this Hirota operator equation is sometimes called the ‘complex modified Korteweg-de Vries equation [27,28], but this label is misleading, since it is in the NLS family, not the KdV family). A real solution of the Hirota equation will also solve the mKdV. Some solutions, mainly with zero background have been given for α set to -1 in references [29,30]. If ψ is a solution of the defocussing mKdV, $\psi_x + \psi_{ttt} - 6\psi^2\psi_t = 0$, then the Miura transformation [31], $\phi = \psi_t + \psi^2$, is a solution of the KdV, $\phi_x + \phi_{ttt} - 6\phi\phi_t = 0$. This is not the case we deal with here. Both equations are integrable and have infinitely many conserved quantities [32].

The mKdV admits a scaling transformation. Namely, if $\psi = \psi(x, t)$ is a solution of equation (1), then

$$\psi' = q\psi(q^3x, qt) \quad (2)$$

is also a solution of equation (1) for arbitrary real q . For example, for the basic soliton solution $\psi = \text{sech}(t + \alpha x)$, the extended one-parameter family of solutions can be

^a e-mail: huqemdad@gmail.com

written as $\psi = q \operatorname{sech}(qt + \alpha q^3 x)$, where q is an arbitrary real number. This scaling applies to all mKdV solutions including those given in this work. We will provide solutions with $q = 1$ as unit-background solutions. The mKdV can also be written in the form of the continuity equation [33]:

$$\frac{\partial \psi}{\partial x} = \frac{\partial}{\partial t} [\alpha (\psi_{tt} + 2\psi^3)].$$

In contrast to KdV, the mKdV equation is not invariant under Galilean transformation.

Explicit solutions of the mKdV have been derived using various methods. For instance, Hirota derived the exact envelope soliton for the mKdV equation in reference [34] and for multiple collision of solitons with different amplitudes in reference [35]. The inverse scattering technique (IST) has been developed to solve a range of nonlinear evolution differential equations, including the mKdV equation in reference [36]. The IST for the mKdV equation was given by Tanaka [37]. Wadati used the IST to obtain the exact N -soliton solution for the mKdV [38]. Direct methods can also be used to derive certain solutions. Some classes of periodic solutions of mKdV have been derived in [39]. In this work, using a Darboux transformation with seeding solution $\psi = 1$, we derive exact periodic and rational solutions. These correspond to imaginary eigenvalues of the IST.

The Lax-pair for the mKdV equation was given by Wadati [38]. We note that Wadati used the opposite sign for α . Our notation below is adapted to equation (1). Now, two linear equations

$$\begin{aligned} \frac{\partial R}{\partial t} &= UR, \\ \frac{\partial R}{\partial x} &= VR, \end{aligned} \quad (3)$$

are such that the ‘zero-curvature’ condition:

$$U_x - V_t + [U, V] = 0, \quad (4)$$

will reproduce equation (1). Here U and V are 2×2 matrices with U given by

$$U = i \begin{bmatrix} \lambda & \psi(x, t)^* \\ \psi(x, t) & -\lambda \end{bmatrix}, \quad (5)$$

while V is a matrix polynomial in eigenvalue λ . For the mKdV, it is a simple cubic polynomial that can be written in general form $V = \alpha \sum_{j=0}^3 \lambda^j V_j$, where submatrices V_j are

$$V_j = i \begin{bmatrix} A_j & B_j^* \\ B_j & -A_j \end{bmatrix}, \quad (6)$$

with

$$\begin{aligned} A_0 &= -i (\psi_t^* \psi - \psi_t \psi^*), \\ B_0 &= 2\psi^2 \psi + \psi_{tt}, \\ A_1 &= 2\psi^2, & B_1 &= -2i\psi_t, \\ A_2 &= 0, & B_2 &= -4\psi, \\ A_3 &= -4, & B_3 &= 0. \end{aligned}$$

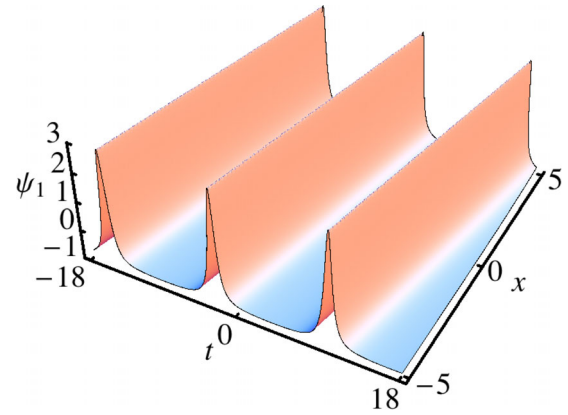


Fig. 1. A first order mKdV periodic solution equation (7) with $\lambda = 0 + 0.97i$ (or $\kappa = 0.48621$) and $\alpha = -\frac{1}{10}$. Here, the amplitude remains constant.

It is easy to check that substitution of the matrices U and V into equation (4) leads directly to equation (1).

2 First-order periodic and rational solutions

Using the seeding solution $\psi = 1$, the imaginary eigenvalue $\lambda = ib$ and the same basic steps as in [40], we obtain the periodic solution of the mKdV:

$$\psi_1 = -1 + \frac{\kappa^2}{2 - \sqrt{4 - \kappa^2} \cos[\kappa(t + vx)]}, \quad (7)$$

where $\kappa = 2\sqrt{1 + \lambda^2}$ and $v = \alpha(6 - \kappa^2)$. Thus we need $\kappa < 2$. This solution is shown in Figure 1. In contrast to the Akhmediev breather of the nonlinear Schrödinger equation (NLSE) [41,42], which is localized in x and periodic in t , this mKdV solution is periodic in t but maintains constant amplitude of oscillations $\sqrt{4 - \kappa^2}$ everywhere. The oscillations move with velocity v in the (x, t) -plane. The solution of equation (7) is real and contains a trigonometric function only. Here, κ is the frequency of the periodic function.

An asymptotic reduction from the modified Korteweg-de Vries equation produces the NLS equation [43,44]. So modulation instability can occur for some parameter values, and an almost periodic wave-train can provide short term pulses of relatively high energy. Figure 1 shows a periodic pattern with the frequency $\kappa = 2\sqrt{1 - b^2} < 2$. The eigenvalue is $\lambda = ib$ where b is real. Then the period of the solution is $T = \pi/\sqrt{1 - b^2}$ along the t axis. Periodic solutions exist for $0 < b < 1$ and consequently their frequencies remain within $0 < \kappa < 2$.

The longest oscillation period of these solutions occurs in the limit $\kappa \rightarrow 0$.

Similar to the case of an Akhmediev breather that becomes a rogue wave [45,46] in the limit $\kappa \rightarrow 0$, the mKdV periodic solution of equation (7) in the same limit, $\kappa \rightarrow 0$, becomes a rational soliton:

$$\psi_1 = -1 + \frac{4}{1 + 4(t + 6x\alpha)^2}. \quad (8)$$

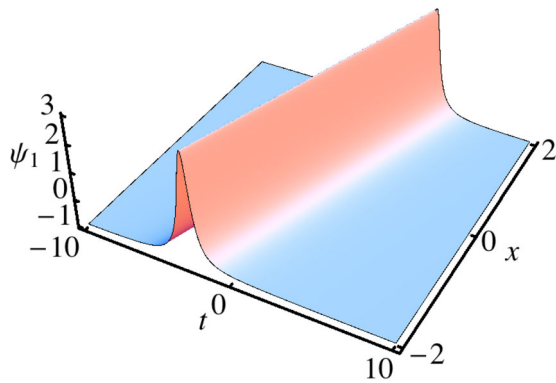


Fig. 2. A first order mKdV rational solution equation (8) with $\alpha = -\frac{1}{4}$.

This corresponds to the Peregrine solution of the NLSE [47,48]. Adding to the similarity, the highest amplitude of the solution is 3, just as occurs with the Peregrine solution. However, instead of being doubly localized, the solution of equation (8) looks more like a soliton on a constant background, $\psi = -1$, moving with velocity v in the (x, t) plane, as shown in Figure 2. Both solutions, equations (7) and (8) lack phase evolution which is an essential part of any NLSE solution. This is in accordance with the fact that the mKdV directly describes the wave profile rather than a wave envelope function. These solutions are reminiscent of the periodic ‘cnoidal’ waves of the NLSE, as discussed in [49].

3 Second order periodic solution

The second step in the Darboux transformation scheme [40] provides us with the second-order periodic solution of the mKdV equation:

$$\psi_2 = 1 + \frac{N_2}{D_2}, \tag{9}$$

where

$$\begin{aligned} N_2 &= (v_1^2 - v_2^2)[v_2(v_1 \cos F_1 - 2)(2 \cos F_2 - v_2) \\ &\quad - v_1(2 \cos F_1 - v_1)(v_2 \cos F_2 - 2)] \\ D_2 &= -2v_1v_2\{\kappa_1\kappa_2 \sin F_1 \sin F_2 \\ &\quad + [2 \cos F_1 - v_1][2 \cos F_2 - v_2]\} \\ &\quad + (\kappa_1^2 + \kappa_2^2 - 8)[2 - v_1 \cos F_1][v_2 \cos F_2 - 2], \end{aligned}$$

and

$$\begin{aligned} F_1 &= x\alpha\kappa_1(6 - \kappa_1^2) + t\kappa_1, \\ F_2 &= x\alpha\kappa_2(6 - \kappa_2^2) + t\kappa_2, \\ v_1 &= \sqrt{4 - \kappa_1^2}, \quad v_2 = \sqrt{4 - \kappa_2^2}. \end{aligned}$$

Here, the maximum value is $1 + v_1 + v_2$ and the minimum value is $1 - v_1 - v_2$. So, the sum of the maximum and minimum values is always 2, independent of α , and the

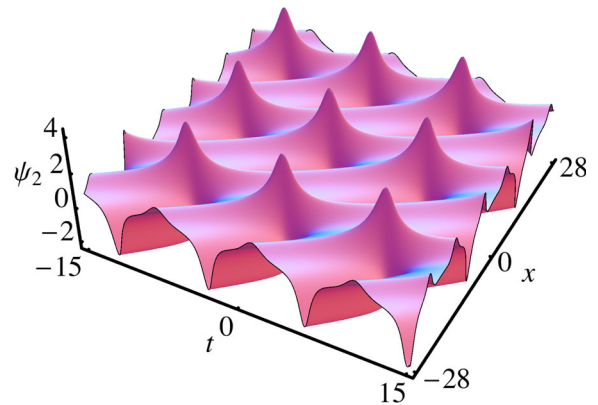


Fig. 3. A second order periodic mKdV solution equation (9) with $\kappa_1 = 0.7$, $\kappa_2 = 1.4$ and $\alpha = -\frac{1}{6}$.

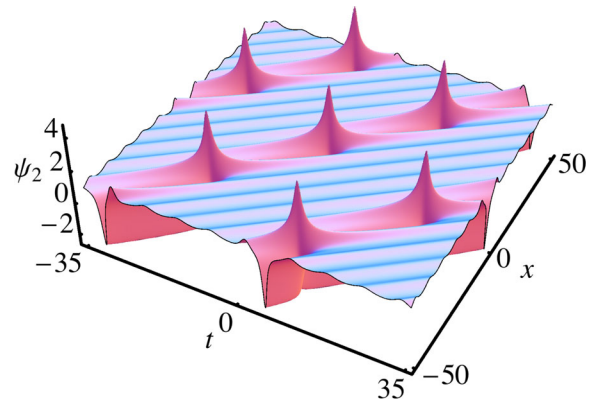


Fig. 4. A second order mKdV solution equation (9) with $\kappa_1 = 0.98$, $\kappa_2 = 0.8$ and $\alpha = -\frac{1}{6}$.

total structure always has height of $2(v_1 + v_2)$. The solution is shown in Figure 3. This is the nonlinear superposition of the set of two periodic solutions obtained in the previous step crossing each other. Thus, the solution creates the two-dimensional ‘lattice’. Each individual wave train has specific values of frequencies, κ_1 and κ_2 , respectively. The maximum amplitude of the superposition is 4.30, while the minimum one is -2.30 . The maxima of the lattice appear at the positions of intersection of troughs of one periodic structure with the maxima of the other one. This happens with all second-order solutions below.

Figure 4 shows another example of a second order doubly-periodic solution with different values of κ_1 and κ_2 . The velocities of propagation of the two individual solutions, $\alpha(6 - \kappa_1^2)$ and $\alpha(6 - \kappa_2^2)$, are now closer to each other. Thus, the two periodic structures comprising the lattice are located at smaller angles to each other. Their periods differ significantly. In Figure 4, the maximum amplitude is 4.57 and the minimum is -2.57 .

The frequencies of the individual components, κ_1 and κ_2 , in the above solutions must remain within the range $0 < \kappa_1, \kappa_2 \leq 2$. When we have $\kappa_i \rightarrow 2$ for either one, the corresponding solution reduces to a constant amplitude background wave.

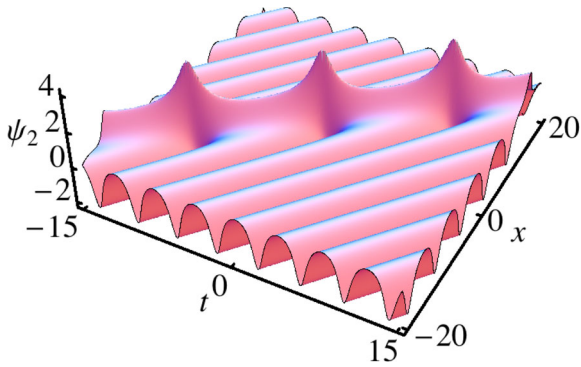


Fig. 5. A second order mKdV solution equation (10) with $\kappa_1 = 1.6$ while $\kappa_2 \rightarrow 0$ and $\alpha = -\frac{1}{6}$.

Either of the frequencies, κ_1 or κ_2 , in the solution can be zero. When $\kappa_2 = 0$, the solution is:

$$\psi_2 = 1 - \frac{\kappa_1^2}{D_3} [-8 + 4v_1 \cos(R_1) + (1 + 4p_1^2) \kappa_1^2], \quad (10)$$

with

$$D_3 = -16p_1^2 (v_1^2 - 4) - 16p_1 v_1 \kappa_1 \sin(R_1) + 4[4 - 4v_1 \cos(R_1) + v_1^2] + (1 + 4p_1^2) [v_1 \cos(R_1) - 2] \kappa_1^2$$

where

$$R_1 = (t - V_b x) \kappa_1, \quad p_1 = t + 6\alpha x \\ V_b = \alpha (-6 + \kappa_1^2).$$

The solution is significantly simplified and contains a rational component and only one wave frequency. This solution is shown in Figure 5. The background here has only one periodic component. The presence of the rational component is revealed in a single ridge of higher amplitudes crossing the origin. The solution is also periodic along this line, as the ridge crosses the periodic background at a finite angle. The periodicity of the maxima along the ridge is defined by this angle. The maximal amplitude of periodic field variation along this line is 4.2.

4 Degenerate solution

Generally, the inverse scattering technique does not allow the presence of two equal eigenvalues in the solution. The solution becomes undefined when $\lambda_1 \rightarrow \lambda_2$, or, equivalently $\kappa_1 \rightarrow \kappa_2$. Despite having this restriction, it is still possible to derive the solution in this limiting case. To proceed with the derivation, we set $\kappa_2 \rightarrow \kappa_1 + \epsilon$. Then, we take a Taylor series expansion of this expression in terms of ϵ and retain only the lowest order terms. This leaves us with a real second order degenerate mKdV solution:

$$\psi_2 = 1 + \frac{N_d}{D_d}, \quad (11)$$

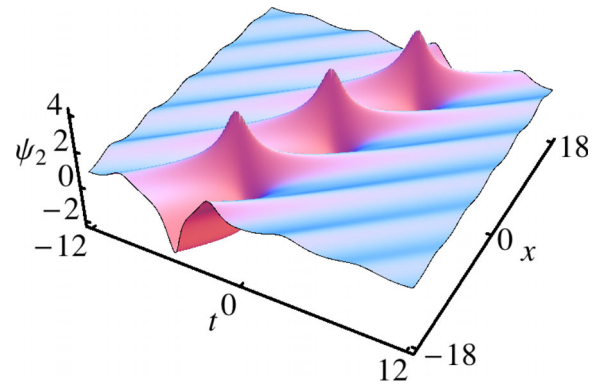


Fig. 6. A second order degenerate mKdV solution, equation (11), with $\kappa = 1.2$ and $\alpha = -\frac{1}{6}$.

where

$$N_d = 4\kappa^2 v_a^2 \times \{ \kappa v_a^2 [t - 3\alpha(\kappa^2 - 2)x] \sin R_b - (\kappa^2 - 8) \cos R_b - 4v_a \}$$

and

$$D_d = -8\kappa v_a^4 [t - 3\alpha(\kappa^2 - 2)x] \sin R_b - v_a^5 \cos(2R_b) - 8\kappa^2 v_a^2 \cos R_b - v_a \{ -2\kappa^6 (t^2 + 60\alpha t x + 468\alpha^2 x^2) + 12\alpha \kappa^8 x (t + 18\alpha x) + \kappa^4 [16(t + 6\alpha x)(t + 18\alpha x) + 1] - 8\kappa^2 [4(t + 6\alpha x)^2 + 1] - 18\alpha^2 \kappa^{10} x^2 - 16 \},$$

with

$$v_a = \sqrt{4 - \kappa^2}, \quad V_b = \alpha (\kappa^2 - 6), \\ R_b = (t - V_b x) \kappa,$$

here, $\kappa = \kappa_1 = \kappa_2$. An example of this degenerate solution of the mKdV is presented in Figure 6. The wave pattern of this solution consists of a single periodic ridge of high amplitude peaks on a periodic wave background. The background modulation is much weaker than the modulation along the periodic ridge. The maximum amplitude of the peaks along the ridge is $(\psi_2)_{\max} = 5$. The line of peaks crosses the origin. The positions of the peaks are synchronised with the periodic wave structure of the background.

5 Second-order rational solution

We can further simplify the solution of equation (10) by taking the other frequency $\kappa_1 \rightarrow 0$. Trigonometric functions then disappear and we obtain the second-order purely rational solution of mKdV equation:

$$\psi_2 = 1 + 12 \frac{G_2}{D_2}, \quad (12)$$

where

$$G_2 = 3 - 8(6\alpha x + t) [2(6\alpha x + t)^3 + 3(22\alpha x + t)]$$

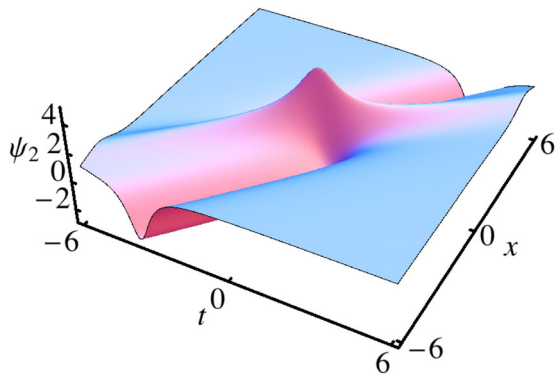


Fig. 7. A second order mKdV rational solution equation (12) with $\alpha = -\frac{1}{6}$.

and

$$D_2 = 48\alpha x \left[62208\alpha^4 x^4 (\alpha x + t) + 432\alpha^3 (60t^2 - 13)x^3 + 288\alpha^2 t (20t^2 - 9)x^2 + 3\alpha (240t^4 - 120t^2 + 139)x + t (48t^4 - 8t^2 + 51) \right] + 64t^6 + 48t^4 + 108t^2 + 9.$$

This solution is shown in Figure 7. The solution is real without any periodicity and is located on a flat background, $\psi = 1$. The solution is seemingly a result of a collision of a dip and a bright soliton with slightly different velocities. The collision point is at $(0, 0)$ and has a single peak with the highest amplitude 5 at the origin. Remarkably, this value is the same as for the second-order rogue wave of the NLSE [42,50,51]. This solution is a proof that the mKdV also has a high-amplitude rational solution localized in two dimensions. The depressed soliton part of this solution has a minimum around -2.75 , thus making the central part of the solution significantly higher than the bottom of the trough.

Returning to the simple scaling of equation (2), we note that the rational solution can be transformed to arbitrary background a and arbitrary maximal amplitude $5a$. Then it is given by

$$\psi_2 = a \left(1 + 12 \frac{G'_2}{D'_2} \right), \tag{13}$$

where each x is replaced by $a^3 x$ and each t by at in the above expressions for G_2 and D_2 . Thus,

$$G'_2 = 3 - 8a (6a^2\alpha x + t) \times \left[2a^3 (6a^2\alpha x + t)^3 + 3a (22a^2\alpha x + t) \right]$$

and similar modification applies for D'_2 .

6 Second order rational solution with differential shift

Continuing the comparison with the rogue wave solutions of the NLSE, we recall that, for the NLSE equation, a

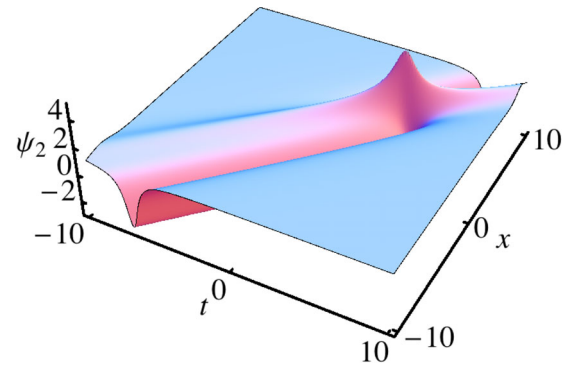


Fig. 8. A second order mKdV rational solution, equation (14), with shift parameter $c_a = -2$; here $\alpha = -\frac{1}{6}$.

form of the second-order rogue wave solution appears as a triplet of well-separated first-order rogue waves [52,53]. This form requires two additional free parameters that move the rogue wave components out from the centre of the structure. We call these parameters “differential shifts” [23,54,55]. They should not be confused with trivial translations along the x and t co-ordinates. In contrast to the NLSE equation, the mKdV rational solution cannot be split into three components, as there are no first-order rational solutions here. We apply the “differential shifts”, x_d and t_d , to the solution of equation (12) in the same way as in [23,54].

We set $c_a = x_d + 6\alpha t_d$ as the combined constant. We find:

$$\psi_2 = 1 + \frac{N_t}{D_t} \tag{14}$$

where

$$N_t = -12\{8(t + 6\alpha x)[-16c_a + 2t^3 + 6\alpha(6t^2 + 11)x + 216\alpha^2 t x^2 + 3t + 432\alpha^3 x^3] - 3\},$$

and

$$D_t = 4\{256c_a^2 + 3456\alpha^3 x^3(8c_a + 20t^3 - 9t) + 36\alpha^2 x^2[24t(16c_a + 10t^3 - 5t) + 139] + 128c_a t^3 + 12\alpha x(192c_a t^2 - 176c_a + 48t^5 - 8t^3 + 51t) - 96c_a t + 16t^6 + 12t^4 + 5184\alpha^4(60t^2 - 13)x^4 + 27t^2 + 3(12\alpha x)^5(t + \alpha x)\} + 9.$$

Now, the new solution, equation (14), has a free real parameter, c_a . For $c_a = 0$, the solution equation (14) coincides with the second-order rational solution of equation (12). Two examples of this solution with nonzero values of x_d and t_d are shown in Figures 8 and 9.

As we can see, the action of these parameters on the rational solution results in a shift of the peak of along the “depressed soliton” trough. This is different from elementary translations of the solution along the x and t axes. In the present case, the translation is eigenvalue-dependent.

7 Conclusion

In our work, we have found new periodic solutions of the mKdV equation. A second order nonlinear superposition

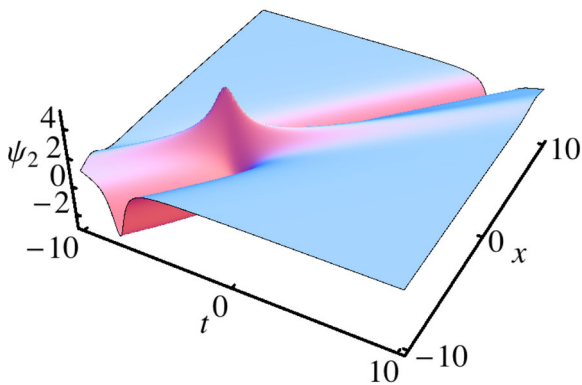


Fig. 9. A second order mKdV rational solution, equation (14), with shift parameter $c_a = 2$; here $\alpha = -\frac{1}{6}$.

of them, constructed with the use of the Darboux transformation, leads to doubly-periodic “lattice”-type structures. Limiting cases of these structures include a high-amplitude oscillating ridge on a single periodic background, soliton-like structures and, most remarkably, a rational solution on a constant background with an infinitely extended “depressed soliton” trough.

Breathers and rogue wave solutions of the NLSE are used mainly to explain wave dynamics in deep water and optical pulse dynamics in nonlinear optics. The corresponding classes of solutions of the mKdV equation derived in this work are fundamentally different from those of the NLSE. The solutions of the mKdV are related to the wave profile directly. These solutions reveal that the phenomena of breathers and rogue waves are not confined to the deep ocean. Being the rational solutions of the mKdV equation, they may appear in electromagnetic waves in quantized films, internal waves for some density stratifications, elastic media [56] as well. Remarkably, in the deep ocean, modulation instability contributes to the formation of rogue waves through NLSE breather dynamics, while, in the shallow water case, we obtain rational solutions and solitons in the zero frequency limit ($\kappa \rightarrow 0$) of mKdV solutions. Hence, the deep and shallow water cases provide two different descriptions in hydrodynamics.

These new solutions will undoubtedly be useful and will give insight in modelling nonlinear wave processes in various other physical systems where the mKdV is relevant.

Author contribution statement

A.C. derived all the solutions and generated all the figures. All authors equally contributed to prepare the manuscript.

The authors acknowledge the support of the Australian Research Council (Discovery Project number DP140100265). N.A. and A.A. acknowledge support from the Volkswagen Stiftung and A.C. acknowledges Endeavour Postgraduate Award support and support from a Ben Williams student grant.

References

1. J. Scott Russell, in *14th meeting of the British Association for the Advancement of Science, 1844*, Vol. 311, p. 390
2. Lord Rayleigh, *Phil. Mag.* **1**, 257 (1876)
3. J. Boussinesq, *Essai sur la Théorie des Eaux Courantes* (Imprimerie Nationale, Paris, 1877)
4. J. Boussinesq, *C. R. Acad. Sci.* **72**, 755 (1871)
5. J. Boussinesq, *J. Math. Pure Appl.* **17**, 55 (1872)
6. J. Boussinesq, *C. R. Acad. Sci.* **73**, 256 (1871)
7. D.J. Korteweg, G. De Vries, *The London, Edinburgh, and Dublin Philos. Mag. J. Sci.* **39**, 422 (1895)
8. N.J. Zabusky, M.D. Kruskal, *Phys. Rev. Lett.* **15**, 240 (1965)
9. C.S. Gardner, J.M. Greene, M.D. Kruskal, R.M. Miura, *Phys. Rev. Lett.* **19**, 1095 (1967)
10. H. Leblond, D. Mihalache, *Phys. Rev. A* **79**, 063835 (2009)
11. H. Leblond, D. Mihalache, *J. Phys. A* **43**, 375205 (2010)
12. H. Leblond, D. Mihalache, *Rom. Rep. Phys. Suppl.* **63**, 1254 (2011)
13. H. Leblond, Ph. Grelu, D. Mihalache, *Phys. Rev. A* **90**, 053816 (2014)
14. H. Ono, *J. Phys. Soc. Jpn* **61**, 4336 (1992)
15. A.H. Khater, O.H. El-Kalaawy, D.K. Callebaut, *Phys. Scr.* **58**, 545 (1998)
16. E.A. Ralph, L. Pratt, *J. Nonlinear Sci.* **4**, 355 (1994)
17. T.S. Komatsu, Shin-ichi Sasa, *Phys. Rev. E* **52**, 5574 (1995)
18. Z.-P. Li, Y.-C. Liu, *Eur. Phys. J. B* **53**, 367 (2006)
19. H.X. Ge, S.Q. Dai, Y. Xue, L.Y. Dong, *Phys. Rev. E* **71**, 066119 (2005)
20. V. Ziegler, J. Dinkel, C. Setzer, K.E. Lonngren, *Chaos Solitons Fractals* **12**, 1719 (2001)
21. K.E. Lonngren, *Optical and Quantum Electronics* **30**, 615 (1998)
22. M.A. Helal, *Chaos Solitons Fractals* **13**, 1917 (2002)
23. A. Chowdury, D.J. Kedziora, A. Ankiewicz, N. Akhmediev, *Phys. Rev. E* **91**, 022919 (2015)
24. A. Chowdury, D.J. Kedziora, A. Ankiewicz, N. Akhmediev, *Phys. Rev. E* **90**, 032922 (2014)
25. A. Ankiewicz, N. Akhmediev, *Phys. Lett. A* **378**, 358 (2014)
26. A. Ankiewicz, Y. Wang, S. Wabnitz, N. Akhmediev, *Phys. Rev. E* **89**, 012907 (2014)
27. Zhaqilao, *Phys. Scr.* **87**, 065401 (2013)
28. L. Li, K. Porsezian, J. He, L. Wang, R. Erdelyi, *Phys. Rev. E* **89**, 062917 (2014)
29. Sun Ying-Ying, Zhang Da-Jun, *Commun. Theor. Phys.* **57**, 923 (2012)
30. D.-J. Zhang, S.-L. Zhao, Y.-Y. Sun, J. Zhou, *Rev. Math. Phys.* **26**, 1430006 (2014)
31. R.M. Miura, *J. Math. Phys.* **9**, 1202 (1968)
32. R.M. Miura, *SIAM Rev.* **18**, 412 (1976)
33. N.F. Smyth, A.L. Worthy, *Wave Motion* **21**, 263 (1995)
34. R. Hirota, *J. Math. Phys.* **14**, 805 (1973)
35. R. Hirota, *J. Phys. Soc. Jpn* **33**, 1456 (1972)
36. M.J. Ablowitz, D.J. Kaup, A.C. Newell, H. Segur, *Phys. Rev. Lett.* **31**, 125 (1973)
37. Sh. Tanaka, *Proc. Jpn Acad.* **48**, 466 (1972)
38. M. Wadati, *J. Phys. Soc. Jpn* **32**, 1681 (1972)
39. P.G. Kevrekidis, A. Khare, A. Saxena, G. Herring, *J. Phys. A* **37**, 10959 (2004)
40. N. Akhmediev, V.I. Korneev, N.V. Mitskevich, *Zh. Eksp. Teor. Fiz.* **94**, 159 (1988) English translation in: [*Sov. Phys. J. Exp. Theor. Phys.* **67**, 89 (1988)]

41. N. Akhmediev, V.I. Korneev, *Teor. Mat. Fiz.* **69**, 189 (1986). English translation in: [*Theor. Math. Phys.* **69**, 1089 (1986)]
42. N. Akhmediev, V. Eleonsky, N. Kulagin, *Sov. Phys. J. Exp. Theor. Phys.* **62**, 894 (1985)
43. R. Grimshaw, E. Pelinovsky, T. Talipova, M. Ruderman, R. Erdelyi, *Stud. Appl. Math.* **114**, 189, (2005)
44. R. Grimshaw, D. Pelinovsky, E. Pelinovsky, T. Talipova, *Physica D* **159**, 35 (2001)
45. N. Akhmediev, V.M. Eleonskii, N.E. Kulagin, *Theor. Math. Phys. (USSR)* **72**, 809 (1987)
46. N. Akhmediev, A. Ankiewicz, J.M. Soto-Crespo, *Phys. Rev. E* **80**, 026601 (2009)
47. D.H. Peregrine, *Adv. Appl. Mech.* **16**, 9 (1976)
48. B. Kibler, J. Fatome, C. Finot, G. Millot, F. Dias, G. Genty, N. Akhmediev, J.M. Dudley, *Nat. Phys.* **6**, 790 (2010)
49. D.J. Kedziora, A. Ankiewicz, N. Akhmediev, *Eur. Phys. J. Special Topics* **223**, 4362 (2014)
50. N. Akhmediev, A. Ankiewicz, M. Taki, *Phys. Lett. A* **373**, 675 (2009)
51. N. Akhmediev, J.M. Soto-Crespo, A. Ankiewicz, *Phys. Lett. A* **373**, 2137 (2009)
52. P. Dubard, P. Gaillard, C. Klein, V.B. Matveev, *Eur. Phys. J. Special Topics* **185**, 247 (2010)
53. A. Ankiewicz, D.J. Kedziora, N. Akhmediev, *Phys. Lett. A* **375**, 2782 (2011)
54. D.J. Kedziora, A. Ankiewicz, N. Akhmediev, *Phys. Rev. E* **85**, 066601 (2012)
55. D.J. Kedziora, A. Ankiewicz, N. Akhmediev, *Phys. Rev. E* **84**, 056611 (2011)
56. T.R. Marchant, *Phys. Rev. E* **66**, 046623 (2002)